Mathematical modeling and computer simulation of Brownian motion and hybridization of nanoparticle-bioprobe-polymer complexes in the low concentration limit

Árpád Tóth [a,b], Dániel Bánky [a,b], Vince Grolmusz [a,b]
[a] Protein Information Technology Group, Eötvös University,
Pázmány Péter stny. 1/C, H-1117 Budapest, Hungary
[b] Uratim Ltd. InfoPark D, H-1117 Budapest, Hungary

Abstract

A wide variety of nano-biotechnologic applications are being developed for nanoparticle based *in vitro* diagnostic and imaging systems. Some of these systems make possible highly sensitive detection of molecular biomarkers. Frequently, the very low concentration of the biomarkers makes impossible the classical, partial differential equation-based mathematical simulation of the motion of the nanoparticles involved. We address the issue of incubation times for low concentration systems using Monte Carlo simulations. We describe a mathematical model and computer simulation of Brownian motion of nanoparticle-bioprobe-polymer contrast agent complexes and their hybridization to immobilized targets. We present results for the dependence of incubation times on the number of particles available for detection, and the geometric layout of the DNA-detection assay on the chip.

Keywords: Brownian motion, first passage time, incubation time, hybridization, Monte Carlo simulation

1 Introduction

As nano-biotechnology is developing, a multitude of diagnostic and visualization applications are being constructed for fast, reliable, on-site molecular recognition. Several of these applications use nanoparticles, that bind to biomarkers, and the nanoparticles make possible the optical recognition of the biomarker molecules [1], [2], [3], [4], [5], [6], [7], [8].

The high-sensitivity applications in molecular recognition need the reliable modeling of the Brownian motion of the nanoparticles in the reaction chamber [9], [10]. The fast distribution of the nanoparticles is generally needed for the completion of the detection, and it is usually the most time-consuming part of the process. Measures, for improving the fast distribution, such as sonication, cannot be used if it breaks the binding of the biomarker-nanoparticle complex, and simple agitation usually does not help much [11].

In the case of the extremely low concentration of biomarkers, the best choice for the Brownian motion prediction is the stochastic computer simulation, since mathematical models involving concentration-based partial differential equations do not seem to be applicable in the range of several hundred or several thousand biomarker molecules [12].

2 Mathematical modeling of incubation times

Our model is a stochastic counterpart of the continuous model presented in [13]. For quality control we need to estimate the time it takes for a successful hybridization of the nanoparticle marked target to the probe site. This is a random variable which at high concentrations is negligible. However for transport limited systems the estimation of these incubation times is a subtle question.

Let τ be the random variable that successful hybridization took place. Then $\tau \in [t, t+\Delta t]$, if between t and $t+\Delta t$ the target collided with the probe site and a reaction took place. Let P_d be the probability that the target and the probe binds, given that they collide. P_d can be observed from the rate constant of hybridization in the large concentration limit [13].

$$k = \frac{DN_\nu AP_d}{2\Sigma}$$

where D is the diffusion coefficient, N_ν is Avogadro's constant, A is the area of the probe site S, i.e. the reaction site for the immobilized probes, and Σ is the frequency of collisions. The value of this rate constant has been established experimentally by Wetmur and Davidson: $k = 3.5 \times 10^5 \frac{L^{1/2}}{N}$, where N is the complexity of the DNA sequence, and L is the number of nucleotide units [14].

The estimation of the probability that a collision took place in the time interval $[t, t+\Delta t]$ reduces down to the computation of the first hitting time, the first time the target hits the spot. This depends on the original position of the target relative to the probe site, and its probability density function f satisfies the Fokker-Planck equation

$$\frac{\partial f}{\partial t} = \Delta f \qquad (1)$$

and the boundary conditions $f(x) = 0$, for $x \in S$, where S is the probe site, as well as mixed boundary conditions

at the boundaries of the reaction chamber representing the adsorption/reflection properties of the bounding walls.

We are interested in incubation time, the shortest time period over which the probability that at least one nanoparticle labeled biotarget is successfully docked for optical recognition exceeds some prescribed probability p, (usually taken to be 99 %). This incubation time depends on p and the various physical, and chemical parameters of the diagnostic setup. For transport limited systems the hybridization after the first hitting of the probe site by the target is negligible compared with the first hitting time, and the inverse function of the cumulative distribution function of the first hitting time gives a very good approximation of the incubation times.

In one dimension there is a closed form solution of equation (1), but such formulae in higher dimensions are lacking. In 2 and 3 dimensional situations numerical approximations to the analytic solutions for typical probe site arrangements are computationally more expensive than statistically sampling from simulated Brownian motion.

3 Results

We present results for the dependence of incubation times on the number of particles available for detection, and the geometric layout of the DNA-detection assay on the chip.

The first table shows the dependence of the incubation time on N = the number of nanoparticle labeled biotargets in the sample, and the diameter of the nanoparticles.

N	50 nm	75 nm	100 nm
100	502 min	756 min	995 min
1000	86 min	132 min	181 min
10000	12 min	18 min	30 min

Although as explained above closed formula solutions are not available for incubation times, it is nevertheless possible to derive some theoretical results about them. The most important is, that in a fixed cuvette, and with the same number of particles the incubation time is inversely proportional to the diffusion coefficient. The following table illustrates how this information can be used to get a least square correction of our simulated samples. The first row shows incubation times for a sample size M =120 runs, the second row LSQ is the least square correction and the third is the result of a finer simulation using M =12000 samples.

M	50 nm	75 nm	100 nm	150 nm
120	15 min	20 min	22 min	60 min
LSQ	14 min	22 min	29 min	43 min
12000	14 min	20 min	27 min	42 min

Another result that can be derived without knowledge of the exact formula for the incubation time concerns the effect of the placement of the probe site. At the sides, and especially in the corner the incubation times change drastically, (they double near the sidewalls, and quadruple at the corners). This theorem is also confirmed using our simulation program. Figure 1 shows incubations times (without least square corrections) as the function of probe site positions.

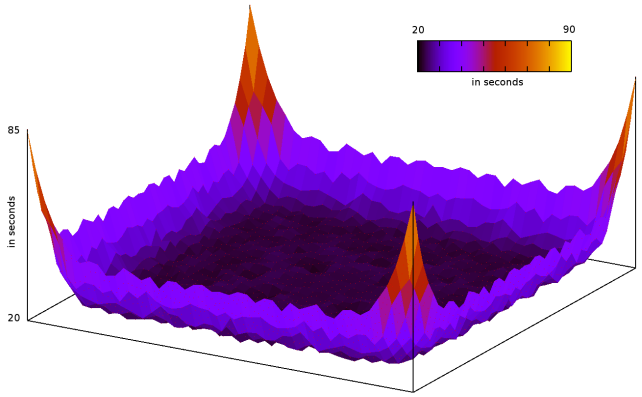

Figure 1: *Incubation times change significantly at the corners.*

Figures 2 and 3 show heat plots of docking ratios as a function of initial positions projected on the front side of the cuvette. Figure 3 shows that within a fixed time period above a certain threshold height no docking will take place.

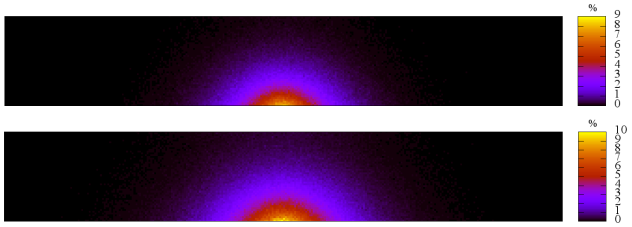

Figure 2: *Heat plot showing ratio of successful docking as a function of the initial position and the effect of ambient temperature, 40 °C (upper), 60 °C (lower).*

4 Methods

Our results were established by a three-dimensional Brownian motion simulation tool for the prediction of the movement of nanoparticles in various thermal, viscosity and geometric settings in a rectangular cuvette.

Our software simulates the movement of an arbitrary number nanoparticles under various, user-selectable circumstances. Each particle is placed randomly and independently with uniform distribution, into the container. Next, random walks are generated for each particle in

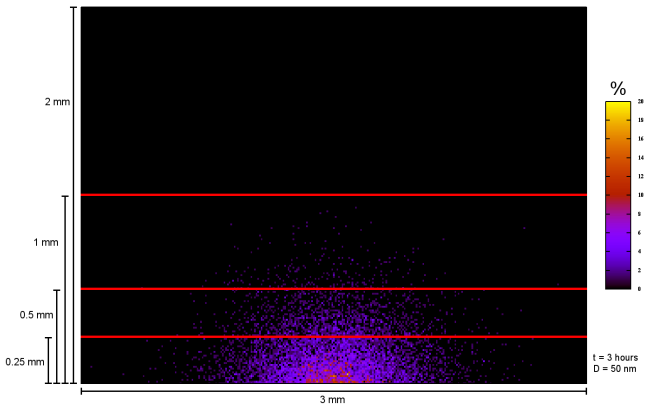

Figure 3: *Heat plot showing ratio of successful docking as a function of the initial position.*

parallel, and the particles keep walking until they hit the target spot on the bottom of the container; if a particle hit the spot, it will not move further: this phenomenon models a (macro-)molecular binding between the spot and the nanoparticle.

The location of the target spot is selectable anywhere in the container. Figure 4 shows the movement of one particle over 3 hours.

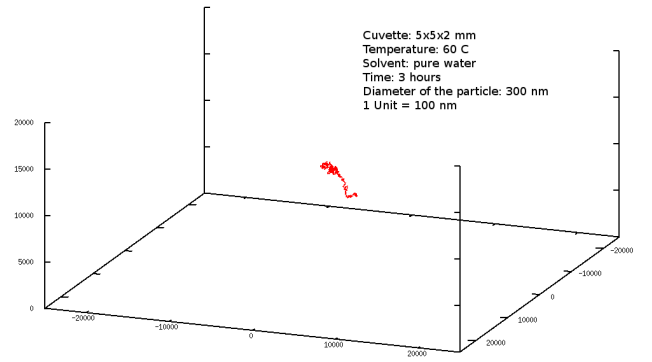

Figure 4: *The simulated movement of a particle over a three hour period.*

The simulation returns the docking ratio and the time needed for docking the very first particle in each experiment. The latter is more relevant measure of success than the former if the docked particles are detected by some qualitative, sensitive method. Heat diagrams for the spatial distribution of the docked ratio are also supplied.

The main *technical novelty* of our solution is the dual time-step approach: while the nanoparticle is far from the target spot, we simulate its movement in larger time steps, and when if it is close to the target spot, we turn to a much finer time step. Note, that the probability distribution of the movements in the rougher time step will be the same as it were simulated in much finer time steps, since the sum of independent normal distributions is normal distribution.

For generating billions pseudorandom numbers of standard normal distribution, we applied the well-known Ziggurat algorithm [15].

Let x, y and z denote independently generated, one-dimensional standard normal distributed pseudorandom variables, resulting from the Ziggurat algorithm. Let $Q = (x, y, z)$ be a three-dimensional vector in normal distribution. Then we generate the simulated Brownian motion of the particle as

$$P_{\texttt{new}} = P_{\texttt{old}} + Q\sqrt{\frac{2}{3}D},$$

where D is the diffusion coefficient, computed from the Einstein-Stokes equation [16]:

$$D = \frac{k_B T}{6\pi\eta r},$$

where k_B is the Boltzmann's constant, η is the viscosity, T is the (absolute) temperature, and r is the radius of the nanoparticle.

In our model, following the model [13], if the particle hits the bottom of the cuvette, it will collide totally elastically with adsorption probability q (i.e., it will continue its 3D movement) and will stick to the bottom plane with probability $1 - q$, to perform a two-dimensional random walk by the rule:

$$P_{\texttt{new}} = P_{\texttt{old}} + Q'\sqrt{D},$$

where $Q' = (x, y)$.

Generating required elementary movements in three dimensional multi-particle Brownian computer simulation, (on the order of tens of millions) for thousands of particles is a very time- and resource consuming computational task. In order to shorten the running time of our program we applied a dual time-step approach:

While the particle is still far from the target spot, we simulate its motion with 1 s time-steps (rough phase). When the particle gets closer than a predefined limit to the spot, we switch to 0.01 s time-steps (fine phase). Figure 5 shows a sample path with these parameters.

Instead of generating 100 random vectors $Q^{(i)}$, $i = 1, 2, \ldots, 100$ with normal distribution with steps of 0.01 s in the rough phase, we just generate one, this improves the running time of the simulation considerably. Note, that the (coordinate-wise) sum of the 100 random vectors

$$\sum_{i=1}^{100} Q^{(i)}$$

has exactly the same distribution as $10(x, y, z)$, where the independent x, y and z have 1-dimensional standard normal distribution.

The simulation of the nanoparticles should be cautious on the border of the rough and the fine phases: it

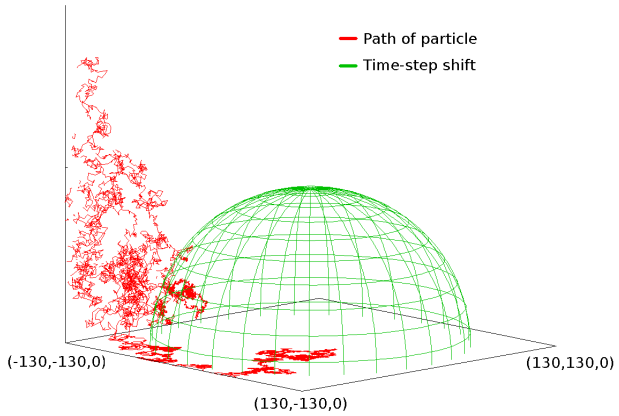

Figure 5: *Coarse and fine simulations change at the green spherical layer.*

may happen that on the border, because of the time-shift, the particles behave strangely. In order to getting rid of this behavior, we change from rough simulation to fine simulation, and back, as follows:

Let R denote the radius of the target spot. When we are closer to the central point of the spot than $5R$, we change from rough simulation to fine simulation. When we move farther from the central point of the spot, than $4R$, we change from fine simulation to rough simulation.

We set up an interactive web server with a slimmed down version of our full featured program. For non-profit users the server is freely available at the site http://brownian.pitgroup.org.

Acknowledgement. The authors acknowledge the partial support of an OTKA grant CNK-77780 and EU FP7 project "NANO-MUBIOP".

REFERENCES

[1] Dongwoo Kim, Weston L Daniel, and Chad A Mirkin. Microarray-based multiplexed scanometric immunoassay for protein cancer markers using gold nanoparticle probes. *Anal Chem*, 81(21):9183–9187, Nov 2009.

[2] Shuang Fang Lim, Robert Riehn, Chih-Kuan Tung, William S Ryu, Rui Zhuo, Joanna Dalland, and Robert H Austin. Upconverting nanophosphors for bioimaging. *Nanotechnology*, 20(40):405701, Oct 2009.

[3] Minghui Xiang, Xiao Xu, Feng Liu, Na Li, and Ke-An Li. Gold nanoparticle based plasmon resonance light-scattering method as a new approach for glycogen-biomacromolecule interactions. *J Phys Chem B*, 113(9):2734–2738, Mar 2009.

[4] Duncan Graham, Karen Faulds, David Thompson, Fiona McKenzie, Robert Stokes, Colette Dalton, Ross Stevenson, Jim Alexander, Paul Garside, and Emma McFarlane. Functionalized nanoparticles for bioanalysis by serrs. *Biochem Soc Trans*, 37(Pt 4):697–701, Aug 2009.

[5] Sarah H Radwan and Hassan M E Azzazy. Gold nanoparticles for molecular diagnostics. *Expert Rev Mol Diagn*, 9(5):511–524, Jul 2009.

[6] Gary M Koenig, Rizal Ong, Angel D Cortes, J. Antonio Moreno-Razo, Juan J de Pablo, and Nicholas L Abbott. Single nanoparticle tracking reveals influence of chemical functionality of nanoparticles on local ordering of liquid crystals and nanoparticle diffusion coefficients. *Nano Lett*, 9(7):2794–2801, Jul 2009.

[7] Hassan M E Azzazy and Mai M H Mansour. In vitro diagnostic prospects of nanoparticles. *Clin Chim Acta*, 403(1-2):1–8, May 2009.

[8] Shiuh-Bin Fang, Wei Yu Tseng, Hung-Chang Lee, Chou-Kun Tsai, Jung-Tang Huang, and Shao-Yi Hou. Identification of salmonella using colony-print and detection with antibody-coated gold nanoparticles. *J Microbiol Methods*, 77(2):225–228, May 2009.

[9] Minh-Phuong Ngoc Bui, Taek Jin Baek, and Gi Hun Seong. Gold nanoparticle aggregation-based highly sensitive dna detection using atomic force microscopy. *Anal Bioanal Chem*, 388(5-6):1185–1190, Jul 2007.

[10] Ye-Fu Wang, Jun-Tao Shen, and Hui-Hui Liu. Analytical performance of and real sample analysis with an hbv gene visual detection chip. *J Virol Methods*, 121(1):79–84, Oct 2004.

[11] Henrik I. Elsner and Erik B. Lindblad. Ultrasonic degradation of dna. *DNA*, 8:697–701, 1989.

[12] Howard C. Berg. *Random Walks in Biology*. Princeton University Press, 1993.

[13] David Erickson, Dongqing Li, and Ulrich J Krull. Modeling of dna hybridization kinetics for spatially resolved biochips. *Anal Biochem*, 317(2):186–200, Jun 2003.

[14] James G. Wetmur, Norman Davidson. Kinetics of renaturation of DNA. *J. Mol. Biol*, 31:349-70. 1968.

[15] George Marsaglia and Wai Wan Tsang. The ziggurat method for generating random variables. *Journal of Statistical Software*, 5(8):1–7, 10 2000.

[16] Albert Einstein. Über die von der molekularkinetischen Theorie der Wärme geforderte Bewegung von in ruhenden Flüssigkeiten suspendierten Teilchen. *Annelen der Physik*, 17:549–560, 1905.